

# Magnetorheological fluid magnetic spring harvester design and characterization

Grazia Lo Sciuto<sup>1</sup>, Joanna Bijak<sup>2\*</sup> , Zygmunt Kowalik<sup>2</sup>, Paweł Kowol<sup>2</sup>

<sup>1</sup> Department of Electrical, Electronics and Informatics Engineering, University of Catania, Viale Andrea Doria 6, 95125 Catania, Italy

<sup>2</sup> Department of Mechatronics, Faculty of Electrical Engineering, Silesian University of Technology, Akademicka 10A, Gliwice 44-100, Poland

\* Corresponding author's e-mail: joanna.bijak@polsl.pl

## ABSTRACT

Magnetic springs are widely investigated as energy converters alternative and energy harvesters by converting mechanical vibrations into electricity at low frequencies. In this article, the design methodology of novel magnetic spring was proposed to improve the dynamic performance and electrical power. The magnetic spring system is composed of a floating magnet and two cylindrical neodymium fixed magnets located on the top and bottom within a cylindrical casing. The external magnets repel the middle (floating) magnet that causes the spring force between them. The advanced magnetic spring system includes a new case with two interior chambers positioned on upper and bottom around the fixed permanent magnets. The chambers are filled with magnetorheological fluid that ensures higher electrical power in comparison to the previous invention in absence of magnetorheological fluid. The general purpose of the realized energy harvester is to provide a novel design of magnetic system with magnetorheological fluid that has the advantages to achieve electrical power in a larger range of frequencies. Additionally, measurements of the displacements and magnetic flux densities have been conducted within a dedicated experimental setup to validate the prototype and its electrical performance.

**Keywords:** magnetic spring, magnetorheological fluid, energy harvesting, displacement, power generation.

## INTRODUCTION

The production, conversion and storage of energy from environment in the natural form of sunlight, wind, waves, tidal and vibrations have been used to power electronic devices, communication systems and IoT (Internet of Things) devices that are characterized with low power consumption [1, 2]. Therefore, the creation of systems that allow accumulating energy are essential for their functioning. The ability to collect the energy necessary to power the electronics of the embedded system from the environment is truly a revolution [3]. However, the technology in production processes is now increasingly oriented towards low-consumption devices and electronic components capable of self-powering from minimum energy achieved by energy harvesters,

such as ultralow-power inverter or compact all-MOSFET [4–6]. Various types of transducers, including electromagnetic, piezoelectric, electrostatic, triboelectric and magnetostrictive, are utilized in mechanical energy harvesters [7, 8]. Mechanical energy harvesters with electromagnetic transducer convert the mechanical motions and vibrations into electrical energy to drive the load through electro-mechanical coupling [9]. Electromagnetic harvesting systems based on magnetic spring are suitable for self-powered technology due to their high efficiency for low-frequency and high-amplitude vibrations, simple design, long-term operation, low production and maintenance costs [10]. These energy harvesting devices consist of fixed and moving magnets as well as coils in magnetic spring [11]. An electromotive force is produced in the coils, according to

Lenz's law, as result of relative motion between the coil and the magnet, depending on the magnetic flux density and the coil parameters [12]. The increase of magnetic flux density is achieved by using more magnets, increasing their size or using other materials. The magnetic spring has a magnetic levitation structure with the basic elements comprising a levitated magnet repelled by fixed magnets. Nevertheless, a more complex design of technological structure can increase energy and power efficiency from the harvester. The physical structure of the hand-held rolling magnetic-spring electromagnetic harvester with configuration of two circular magnets, a cylindrical magnet, three coils, a non-magnetic housing, and a cover is proposed in [13]. Permanent magnets are widely used in vibration harvesters and sensors. Utilization of the negative magnetic spring prototype of energy harvester in order to realize low-frequency vibration energy harvesting and to reduce the resonant frequency of a vibration energy harvester (VEH) was proposed in [14]. The optimal design of magnetic levitation structure in electromagnetic energy harvester for chosen resonance was developed by algorithm in [15]. An enhanced bandwidth nonlinear energy harvester using magnetic spring and magnetic liquid to harvest energy from the vibration environment for energy storage of a low-power device was studied in [16]. To widen the work frequency and enhance output power, the hybrid energy harvester based on flapping wing made of piezoelectric sheet and levitation magnet structure was presented in [17]. To achieve the desired frequency, the electromagnetic energy harvester with adjusting distance between magnets in a Halbach magnet array was designed in [18]. The change of the magnetic spring behavior in energy harvester is achieved by usage of SMART materials. In [19], electromagnetic energy harvester systems were composed of magnets and magnetic fluid that served as damper at high frequencies and as a lubricant at low frequencies. In order to widen the frequency band and improve harvesting efficiency, the ferrofluid around permanent magnets stack acts as its bearing system to minimize any friction during its movement [20]. Smart materials, such as electro- and magneto-rheological (MR) fluids, piezoelectric, shape memory and magnetostrictive materials, are often used in the mechatronic devices due to the controllable properties under the electric or magnetic field and for self-sufficiency of the system

[21]. In particular, MR devices have several applications in the automotive industry, as well as medical and engineering fields for remote control and autonomy [22–24]. MR fluids are mixtures of neutral carrier liquid and ferromagnetic particles.

The MR fluid properties can be controlled by changing the magnetic field [25, 26]. In the absence of an external magnetic field, the magnetic moments associated with each fluid particle, are oriented randomly, and the resulting magnetic force vector is zero. The MR fluid has a constant viscosity coefficient independent of the strain rate. When an external magnetic field is applied, the magnetic moments of the particles align along the magnetic field lines, forming chains. The possibility to control the viscosity of the MR fluid makes it a suitable material for the suspension systems in damping technology, controlling robot movements or receiving the feedback from a manipulator [27–29]. Additionally, the MR fluid is used in the valves, pumps, clutches, brakes and batteries to provide control, lubrication, cooling or energy storage [30–33]. The testing and analysis of MR fluid-filled spring in static and dynamic loading cases have demonstrated that the torsional stiffness of MR fluid inside the spring is dominantly produced due to cross-sectional torsion [34]. The MR fluid-based devices could be considered promising for future application in the energy harvester technology.

The performance of novel devices through design optimization is essential for the engineering application. The new model design suggests the increase of electric power due to the MR fluid effect. A multi-stable magnetic mechanism with a movable permanent magnet and two fixed permanent magnets placed symmetrically on two sides has been used to develop a pendulum vibration energy harvester [35, 36].

The model-based prediction of the magnetic flux density can support the characterization and optimization of the magnetic spring using the design, analysis and measurements [37]. To confirm the usefulness of the magnetic spring, the calculation of the magnetic flux density in a 2D axis-symmetric model has been carried out by simulation analysis and laboratory measurement tests [38, 39]. In addition, the electric circuit has been calculated theoretically using an Finite Element Method (FEM) simulation in ANSYS Maxwell. The measurements of the amplitude of the magnetic spring and vibration generator movement in relation to the frequency were conducted including

the 2-DoF kinematic chain mathematical model of the magnetic spring with spring force and torque, calculated in by the FEM program [40].

This work is focused on a new design concept of magnetic spring with internal chambers containing magnetorheological fluid (MR). The performances of magnetic spring with chambers containing MR fluid strongly depend on frequency range and voltage, providing a great advantage to achieve electric power in an extensive and widespread range of frequencies.

More particularly, the main contributions are summarized as follows:

- The paper proposed a new design and characterization of the magnetic spring with internal chambers containing MR.
- The characterization of magnetic spring was conducted using the experimental set-up, including Hall effect sensors and laser displacement sensors
- The measurements of the magnetic flux density and levitated middle magnet displacement have been conducted in the absence and in the presence of MR fluid contained within the chamber of magnetic spring.
- Electric power was estimated and compared between the new prototypes of magnetic spring in absence and in presence of MR fluid.

## DESIGN OF THE MAGNETIC SPRING

The novel magnetic spring structure was designed for energy harvesting system at the laboratory of Mechatronic Department. The new prototype has involved technical sketches and drawings in Autodesk Inventor Professional 2020 for the 3D construction information. The electrical

and magnetic properties of the 3D printed device in presence and absence of MR fluid as a function of the magnetic field density were investigated. The magnetic structure of a magnetic spring is composed of three neodymium cylindrical magnets enclosed in a casing made of polylactic acid (PLA) material, as shown in Fig. 1d. The Magnetic Spring casing architecture was inspired by the impressive rock-cut of tomb Ramses located at the remote valley known as the Valley of the Kings, in Luxor Egypt (Fig. 1a). The plan of the burial chamber is telescoping from larger to smaller chambers along a central axis with the sanctuary at the end of the sequence. The entrance and corridor of the burial chamber have been designed in the plan of the magnetic spring (Fig. 1b and Fig 1c). The corridor has simple structure and does not have additional branches. On both sides of the corridor there are niches with the reliefs on the walls separated by pillars. The magnetic spring also has a simple, straight structure with similar configuration of niches, as seen in the cross-section of the magnetic spring (Fig. 2a).

In particular, the realized magnetic spring casing has two-chamber housing located in opposite side. The cylindrical housing containing the chambers of the magnetic spring has height of 8 mm, external  $D_{ch}$  and internal  $D_{chin}$  diameter of 15 mm and 9 mm, respectively (Fig. 2a,b). The height  $H_{cas}$  and the outer diameter  $D_{cas}$  of the casing is 31 mm and 17 mm. The assumed dimensions are based on a harvester studied in the earlier work (e.g. in [37–41]). The general size of the device is suited to supply microsensors and MEMS. While the proposed dimensions of the MR magnetic spring might not provide an optimal power production, it is assumed that they are valid enough to ensure proper operation of a

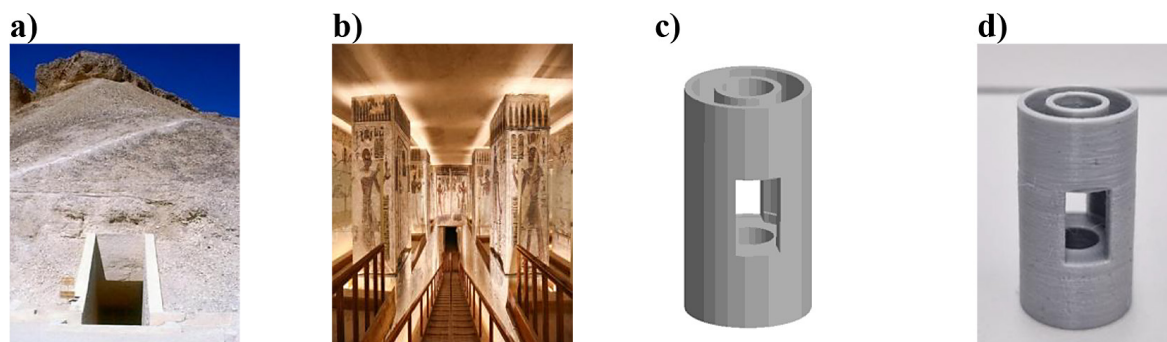


**Figure 1.** (a) Entrance to the tomb of Ramses IV in The Valley of the Kings, also known as the Valley of the Gates of the Kings, in Egypt, (b) Inside a tomb in the Valley of the Kings, (c) 3D models of Magnetic spring casing in Autodesk Inventor Professional, (d) 3D printed model in PLA of magnetic spring casing

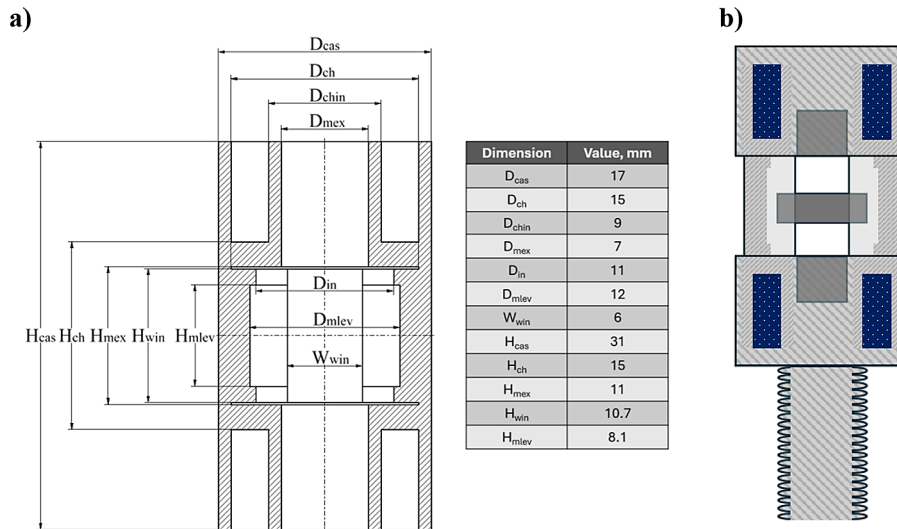


**Figure 2.** Sketch of (a) casing design of magnetic spring with all dimensions expressed in mm and (b) magnetic spring filled of MR fluid

harvester in the presence and absence of MR fluid to explore difference between them.

The chambers (Fig. 3 n. 6) were filled with magnetorheological fluid and sealed using by lids made of PLA material. Casing with chambers and lids (Fig. 3 n. 7, 1 and 4) were printed by means of a Prusa MK3S 3D Printer using grey Filament Noctuo Ultra PLA 1.75 mm with the temperature of the printer bed and the temperature of the filament melting set to 60 °C and 215 °C, respectively. The highest acceleration that acts on the magnetic spring during the test is around 6.8 mm/s<sup>2</sup> with the mass of the magnetic spring of 17.3 g, therefore, force is around 1.18 × 10<sup>-4</sup> N. Durability of the magnetic spring casing was sufficient for the purposes of this test. The magnetic springs in energy harvesters usually work in the lower frequency range, up to 200 Hz; therefore, the risk of layer delamination under higher frequency excitations was not examined. Two identical external permanent magnets with 5 mm of diameters are located on the lids. The lids are designed with a toroidal container (Fig. 3 n. 1 and n. 4 marked

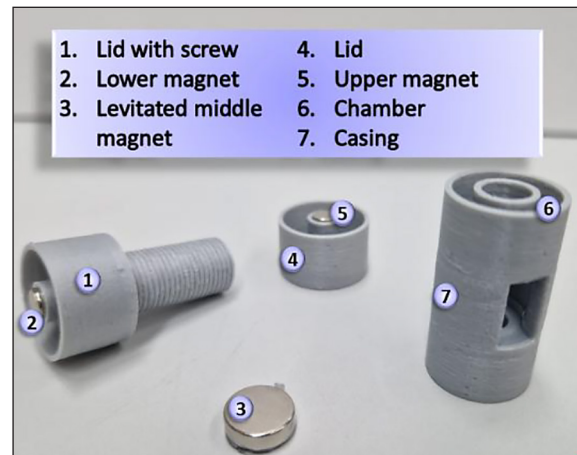


**Figure 3.** Some components as casing, lids, magnets and chambers of the designed MR magnetic spring

in purple) and fixed magnets located as shown in Fig. 3 n. 2 and n. 5. The properties of the magnets are shown in Table 1. Inside the casing, the neodymium disc middle magnet (10 mm of diameter) is placed in repelling configuration with the two fixed magnets. Hence, the middle magnet levitates (Fig. 3 n. 3) between the external magnets and moves provoked by inertial force. This force is caused by the external vibration produced by vibration generator as reported in [41].

**Table 1.** Magnetic and geometrical properties of magnet

Type	<i>m</i> [g]	<i>B<sub>r</sub></i> [T]	<i>H<sub>coB</sub></i> [kA/m] (min.)	<i>H<sub>coJ</sub></i> [kA/m] (min.)	<i>BH</i> max [kJ/m <sup>3</sup> ] (min.)	Height [mm]	Diameter [mm]
External N38	0.74	1.21–1.25	899	955	26	5	5
Middle N38	1.77	1.21–1.25	899	955	26	3	10

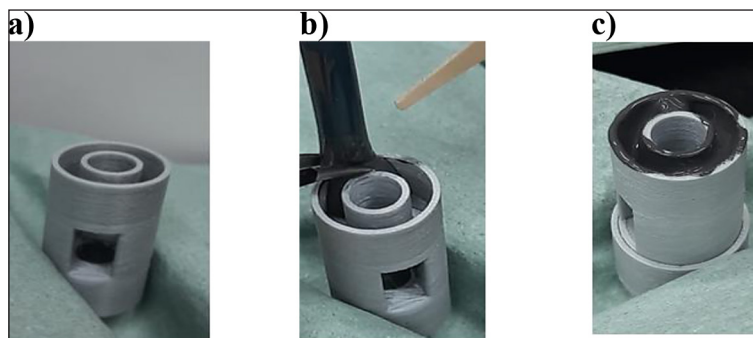


**Figure 4.** The cylindrical housing of magnetic spring: a) in absence of MR fluid b) during the filling stage- injection of MR fluid c) at the final stage of the chamber filled by MR fluid

In the magnetic spring, the chambers were designed to investigate the behavior of controllable MR fluids. The MR fluid was injected inside the chambers using a pre-filled syringe, as shown in the Fig. 4a, b and c. Each chamber was filled with 3 drops (~ 0.68 ml) of MR fluid.

#### BASIC CONCEPT OF MR FLUIDS IN ENERGY HARVESTER MAGNETIC SPRING

A new design of the realized magnetic spring housing and MR fluid located on containers (chambers) is provided for enhancement of the electric power in energy harvesting system. The two permanent magnets are included in the chambers containing the MR exhibiting an air gap.

Usually, a MR fluid is used in various applications utilizing the relation between its viscosity and the magnetic flux density present in the fluid. This allows for controlling its mechanical interaction between certain parts of the machine by means of changing the magnetic flux, usually generated by a coil supplied with a current of controlled value, which is leveraged in the construction of magnetically controlled clutches and dampers. It is worth noting that the process of changing the viscosity in the wide range takes usually a few milliseconds. Another property of MR fluid that is important in the context of a proposed harvester is its magnetic permeability which is approximately equal to 4 and is greater compared to the permeability of PLA or magnets (which is approximately equal to 1). Taking the above into consideration, the assumed influence on the harvester with MR fluid is twofold. First, the addition of MR fluid around the magnet should strengthen and enhance the magnetic flux generated by the magnets. With a careful

coil arrangement, the expected result could be larger amplitude of the voltage induced in the winding and greater power generated by the device. The side effect of such a field amplification should also be the increase of the force acting on a levitated magnet, which in effect increases the stiffness of the magnetic spring and modifies its frequency characteristic by increasing the value of harvester's resonance frequency. The effect of strengthening the magnetic field could also be achieved by using other materials to construct the case of a harvester, either classically used ferromagnetic steels or polymers with ferromagnetic particles. However, in the design process it was decided that the easiest to machine and control option to include ferromagnetic path in the harvester construction is to use the chambers filled with MR fluid.

Such a solution has also one more advantage which brings the second potential benefit of a proposed prototype. During the movement of a harvester, a fluid is allowed to slightly move in the chamber, which increases the overall damping coefficient of the system and extends the amplitude-frequency characteristic of the harvester. For this reason, the harvester can operate and generate energy for vibrations in the wider frequency interval.

Figure 5a shows the SEM image of commercial MR fluid type Lord MRF-132DG (Lord Corporation, Cary, NC, USA) under Digital Microscope Keyence VHX-7000 4K. The MR fluid presents small particles of steel, cobalt, carbon, iron oxide and iron hydroxide (87.3%) wrapped in the organic compound. The micro magnet particles are dispersed in the liquid carrier in the absence of an external magnetic field; their magnetic moments are randomly oriented, and the resultant magnetic force vector is zero. However, when the MR fluid is subjected to external

magnetic field, the particles become magnetized with the moments arranged along the magnetic field force lines (Fig. 5b).

A commercial MR fluid type Lord MRF-132DG (Lord Corporation, Cary, NC, USA) was used In the study. The MR fluid contains small particles of steel, cobalt, carbon, iron oxide and iron hydroxide (87.3%) wrapped in the organic compound. Figure 5a shows the SEM image of this fluid under Digital Microscope Keyence VHX-7000 4K. The behavior of the fluid in an externally induced magnetic field is shown in Figure 5b, where the “spikes” of microparticles formed along the flux lines are visible.

### SIMULATION MODEL

The 2D model of the magnetic spring was designed in Ansys Electronics. Magnetostatic Solver was used to simulate a static magnetic field resulting from the permanent magnets. The

dimensions of the magnets are given in Table 1. The levitated middle magnet is located 4 mm from the upper magnet and from the lower magnet, the magnetic spring is in equilibrium state. The boundary is set to Balloon, which means the region of the model is considered infinitely large. The magnetic coercivity of the magnets is 800 kA/m and relative permeability is 1.0535. The levitated middle magnet is magnetized in z-axis in opposite direction to the upper and lower magnet. The average magnetization characteristic of the MR fluid is nonlinear, and its B-H curve is shown in Figure 6.

The magnetic field distribution in the absence and in the presence of MR fluid is shown in Figures 7 and 8, respectively.

The MR fluid enhances the magnetic flux density  $B$  from maximum of 0.824 T to 0.847 T. It also enhances the area of the significant magnetic flux density value around the magnetic spring. This is useful in terms of the coil placement in the magnetic spring.

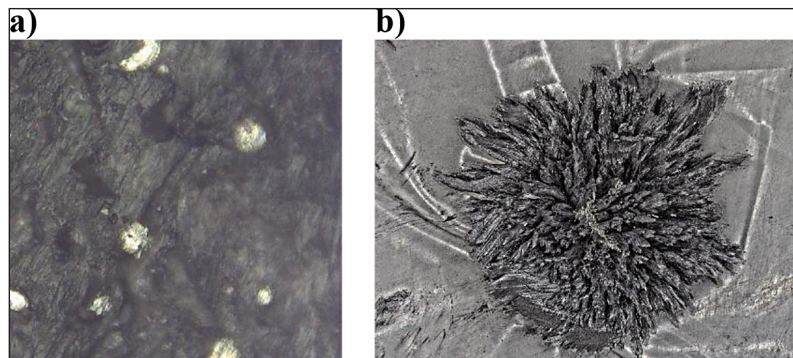


**Figure 5.** The basic performance characterization of MR fluid under the digital microscope: (a) nanoparticles of MR fluid (100 μm), (b) MR particles

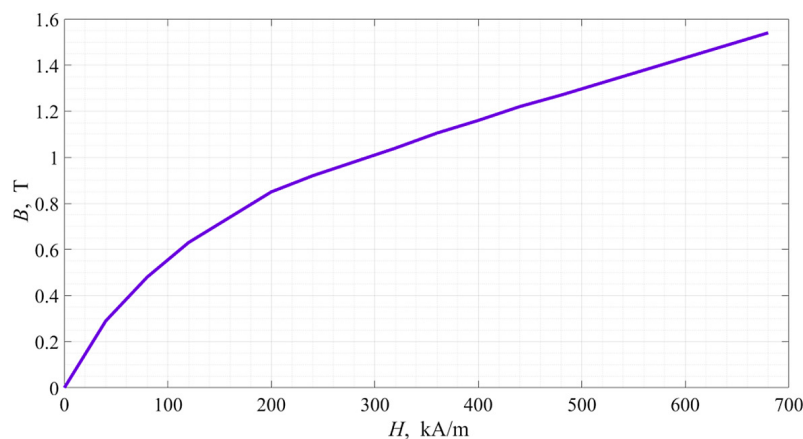


**Figure 6.** B-H curve of the MR fluid

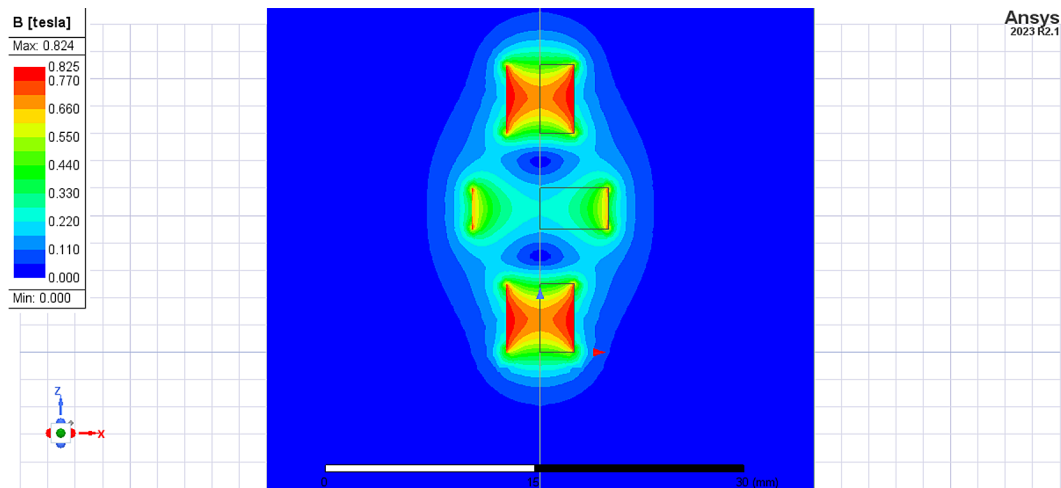


Figure 7. Magnetic field distribution in the absence of MR fluid

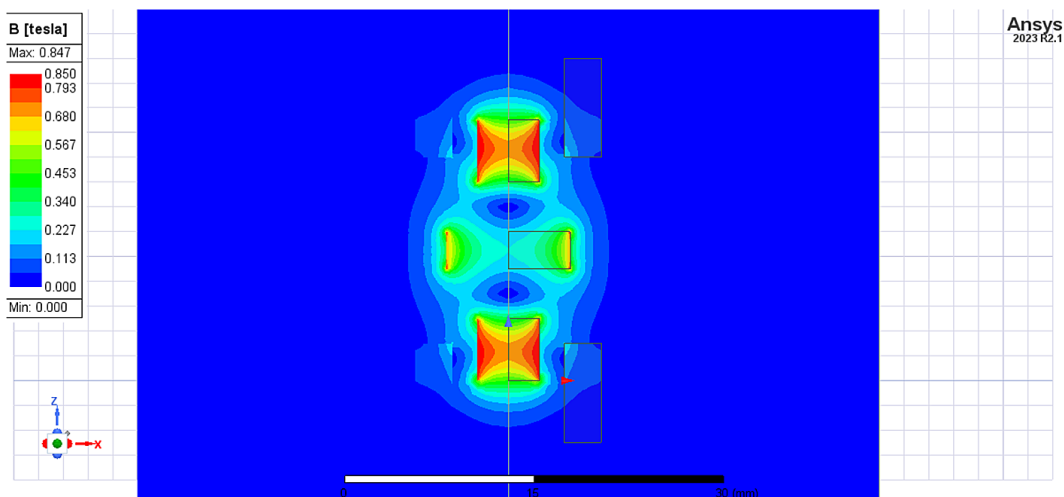


Figure 8. Magnetic field distribution in the presence of MR fluid

## MEASUREMENTS OF MAGNETIC FLUX DENSITY AND DISPLACEMENTS OF MAGNETIC SPRING

The laboratory stand for measurement and analysis of the magnetic and mechanical properties of the designed device is presented in Figure 9 and it comprised a vibration generator to excite the magnetic spring located on top, the function generator, power amplifier, laser heads with panel display, oscilloscopes, power supply, probes and Hall-Effects sensors.

The sinusoidal voltage signal generated by Function Generator Agilent Keysight 33120A is amplified by an FPA200-30W Power Amplifier and supplies the vibration generator. The vibration generator provides external vibrations to the magnetic spring. The Hall-Effects sensors

are located on external casing of the magnetic spring. The structure of the magnetic spring is shown in Figure 10a. Hall-Effect sensors are powered by a Twintex TP-30102 Power Supply with the voltage of 3.3 V. The output magnetic flux density signals are detected by the Hall-Effect sensors placed on the upper, middle and lower part of magnetic spring (Fig. 10b). An LK-G32 Laser Head and an LK-G152 Laser Head controlled by an LK-GD500 display panel collect the signals of the displacements of the magnetic spring and levitated magnet. The output signals were displayed on Tektronix MDO3012 oscilloscopes. The same phases of the signals are achieved by application of the trigger button.

The input voltages were set in the range from 1 V to 6 V due to the mechanical limitation of the

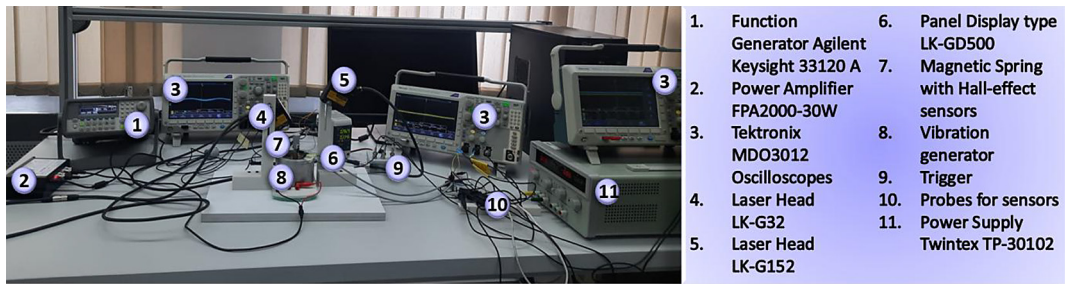


Figure 9. Laboratory stand for the measurement of the magnetic spring properties

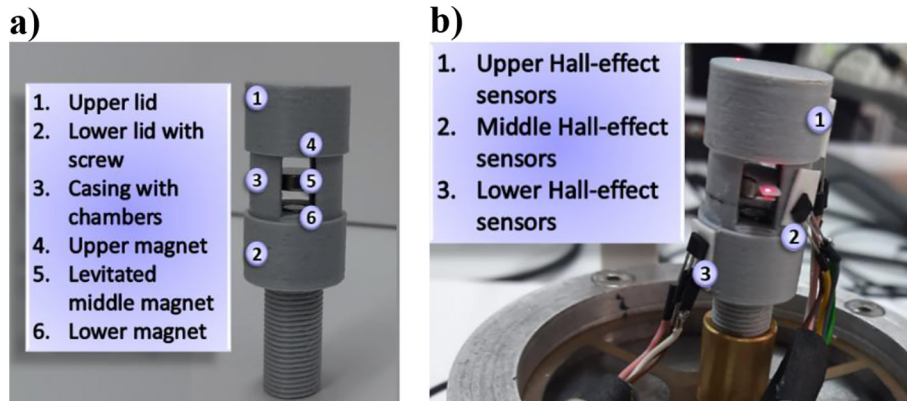


Figure 10. (a) Magnetic spring prototype and description of single parts, (b) magnetic spring prototype on vibration generator during the measurements conducted at the laboratory

vibration generator and the membranes. In particular, the vibrations cause an oscillating motion of the diaphragms made of elastic membrane that under tension can support maximum voltage of 6 V. The frequencies were selected in the range from 5 to 200 Hz. When the magnetic spring is supplied by vibration generator, the levitated magnet generates a magnetic flux that is a combination of the magnetic flux of the permanent magnets and MR fluids magnetic field.

## RESULTS AND DISCUSSION

The experimental procedure and measurements were conducted at the laboratory using the electrical equipment in order to test the MR fluid magnetic spring device. For this purpose, the magnetic spring prototype was analyzed in the absence and in the presence of MR fluid within the chambers of the device. In order to evaluate its performance, the analysis of levitated middle magnet displacement, magnetic flux density for each magnet and electrical power was conducted. The electrical power of the electromagnetic vibration energy harvester depends on the magnetic

flux change during the levitated middle magnet movement. A strong correlation between magnetic flux density and displacement is present in the magnetic spring. The highest electrical power is generated for the highest amplitude of the magnetic flux density and displacements corresponds to the resonance frequency. For this purpose, it is crucial to determine the amplitudes of the displacement and magnetic flux density in function of frequency in magnetic spring system. The input parameters for the supply of vibration generator were defined from 1 to 6 V and for frequency from 0 to 200 Hz. In particular, different range of frequencies from 0 to 50 Hz, from 55 to 135 Hz and from 140 to 200 Hz and voltages were investigated in order to establish the better working operative frequencies and voltages for the MR magnetic spring prototype.

### Displacement of levitated middle magnet in magnetic spring

The displacements of the levitated middle magnet and magnetic spring were measured by the laser distance sensors during the vibration. The displacement of the levitated middle magnet

in the magnetic spring relative to the magnetic spring casing  $d_m$  was determined by Equation 1:

$$d_m = d_{lm} - d_{ms} \quad (1)$$

where:  $d_{lm}$  is the displacement of the levitated middle magnet relative to its initial position and  $d_{ms}$  is the displacement of the magnetic spring relative to its initial position.

The displacement of the levitated middle magnet and displacement of the magnetic spring relative to its initial position in absence and in presence of the MR fluid are shown in Fig. 11a and Fig. 11b, respectively, measured for voltage amplitude of 6 V and frequency of 45 Hz. Due

to the stiff connection between magnetic spring and vibration generator guide, the displacement of the magnetic spring corresponds to the displacement of the vibration generator diaphragm. The displacement of the levitated magnet relative to its initial position is slightly higher in the presence of the MR fluid than in the absence. The amplitude of the levitated middle magnet displacement was calculated by fast Fourier transform (FFT).

*Displacement of levitated middle magnet of magnetic spring device in the absence of MR fluid*

In Figure 12a, for input voltage of 6 V and for frequency of 5 Hz, the highest displacement

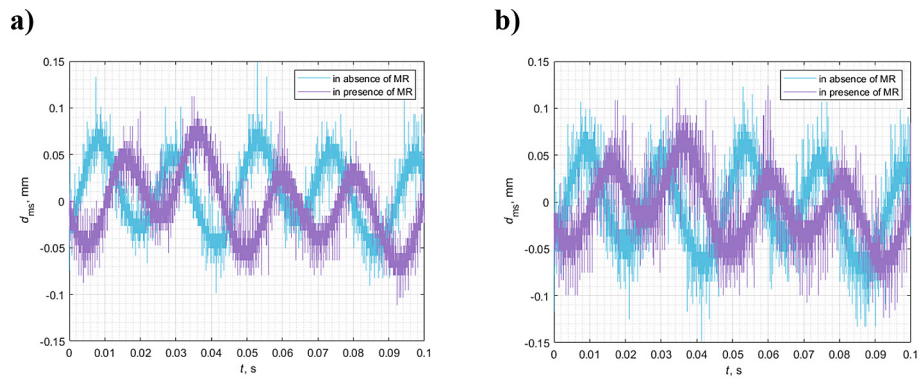


**Figure 11.** The displacement of: (a) the levitated middle magnet relative to its initial position and (b) the magnetic spring relative to its initial position

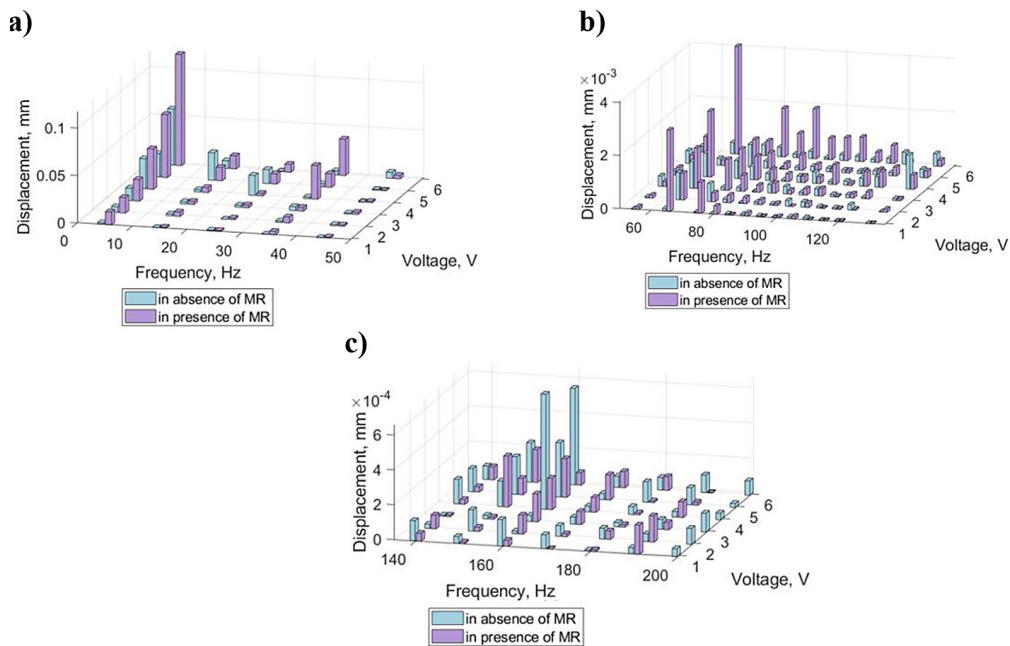


**Figure 12.** The amplitude of the displacement of the levitated magnet in the magnetic spring prototype in the presence and in the absence of MR fluid

is 0.059 mm. In Figure 12b, for input voltage of 2 V and 3 V and for frequency of 65 Hz, the highest displacement is 0.001 mm. In Figure 12c, for voltage of 4 V and for frequency of 160 Hz, the highest displacement is  $6.60 \times 10^{-4}$  mm.

*Displacement of levitated middle magnet of magnetic spring device in presence of MR fluid*

In Figure 12a, for voltage of 6 V and for frequency of 5 Hz, the highest displacement is 0.12 mm. In Figure 12b, for voltage of 6 V and for frequency of 65 Hz, the highest displacement is 0.004 mm. In Figure 12c, for voltage of 4 V and for frequency of 160 Hz, the highest displacement is  $2.92 \times 10^{-4}$  mm. The process of magnetization and demagnetization of magnets affects the displacement of levitated middle magnet with unstable performance, especially in absence of MR fluid in the magnetic spring. However, the opposite behavior is verified in presence of MR fluid achieving the greater stability of the levitated magnet. Thus, the highest value of levitated magnetic displacement is reached in the presence of MR fluid for frequency range from 0 to 120 Hz.

**Magnetic flux density of magnetic spring prototype**

The magnetic flux densities were measured using the Hall-effect sensors and described by FFT.

All effect sensors are linear transducers of the magnetic field and converting it into an electrical signal based on the Hall effect. According to this effect, when a current-carrying conductor or semiconductor is exposed to a perpendicular magnetic field  $B$ , the voltage known as Hall voltage  $V_{HeS}$  is generated across the conductor and is primarily attributed to the Lorentz force acting on the charge carriers within the conductor. The Hall voltage is directly proportional to the product of the current  $I$  flowing through the conductor and the strength of the applied magnetic field  $B$  perpendicular to the current. Magnetic flux density  $B_{mag}$  is calculated using Equation 2:

$$B_{mag} = V_{HeS} c_{HeS} \tag{2}$$

where:  $V_{HeS}$  is the signal voltage of Hall-effect sensors and  $c_{HeS}$  is conversion ratio of 0.43 T/V.

*Magnetic flux density from middle Hall-effect sensor in the absence of MR fluid*

In Figure 13a, for the input voltage of 6 V and for the frequency of 35 Hz, the highest magnetic flux density is 1.95 mT in magnetic spring. In Figure 13b, for the input voltage of 6 V and for the frequency of 55 Hz, the highest magnetic flux density is 2.16 mT. In Figure 13c, for the input voltage of 6 V and for the frequency of 150 Hz, the highest power is 2.26 mT.

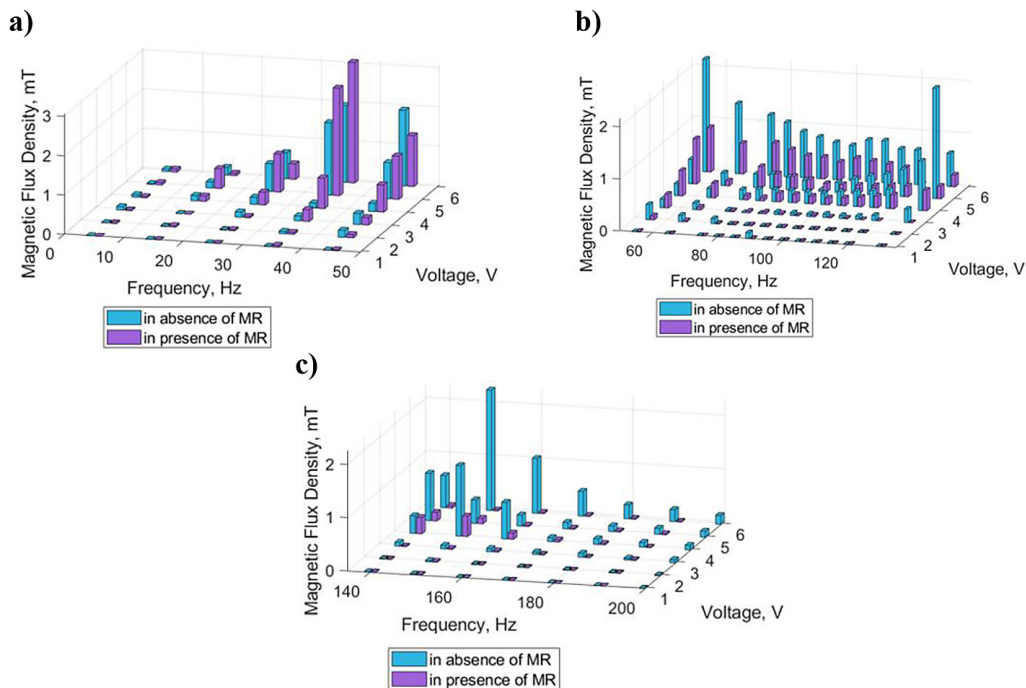


**Figure 13.** The amplitude of the magnetic flux density from the middle Hall-effect sensor

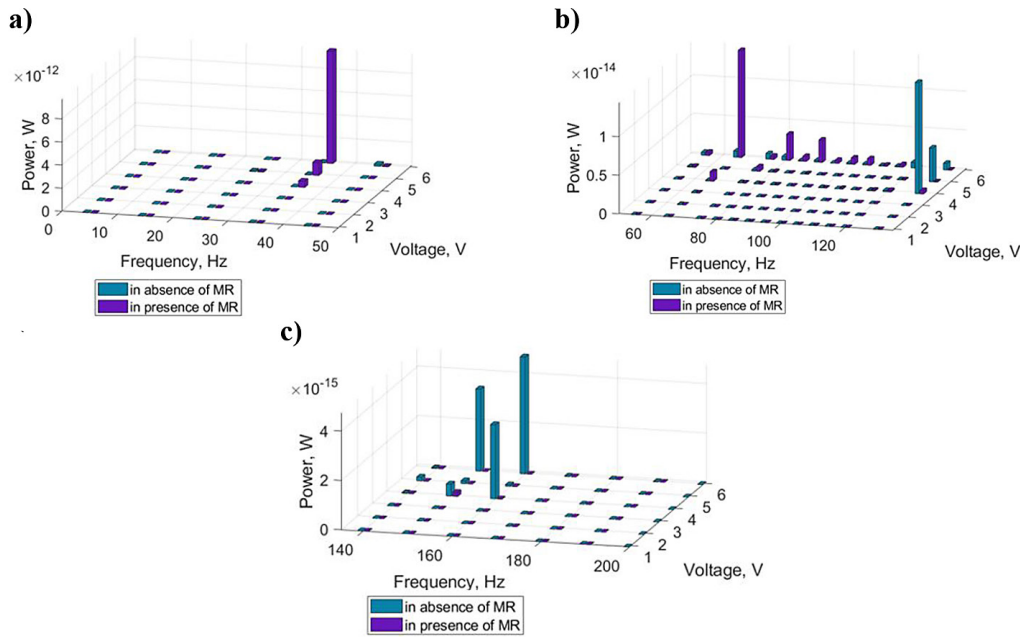


Figure 14. The amplitude of the electrical power of the middle magnet

*Magnetic flux density from middle Hall-effect sensor in the presence of MR fluid*

In Figure 13a, for the input voltage of 6V and for the frequency of 35 Hz, the highest magnetic flux density is 3.07 mT. In Figure 13b, for the input voltage of 5V and for the frequency of 55 Hz, the highest magnetic flux density is 0.87 mT. In Fig. 13c, for the input voltage of 4 V and for the frequency of 150 Hz, the highest power is 0.39 mT. For low frequencies in range from the 0 to 55 Hz and for voltage from 2 to 6 V, the magnetic flux density is higher in presence of the MR fluid. However, good results cannot be extended in the range from 60 Hz to 200 Hz. The maximum magnetic flux density of magnetic spring prototype obtained in the presence of MR fluid is 3.07 mT for the input voltage of 6V and for the frequency of 35 Hz much higher value than 2.26 mT for the input voltage of 6V and for the frequency of 150 Hz in the absence of MR. The MR fluid can positively and successfully affect the magnetic energy efficiency of the prototype useful for future engineering application, especially in the range of frequency from 0 to 60 Hz

**Electrical power of magnetic spring prototype**

The maximum electrical power is obtained by magnetic flux density of the magnets and displacement of the levitated magnet in magnetic spring. To calculate the maximum electrical

power, the magnetic spring with single winding turn coil was considered. The single winding turn coil has radius  $r_{coil}$  of 10 mm wound in the copper wire with area  $S_{wire}$  of  $1.57 \times 10^{-8} \text{ mm}^2$ . The resistance of the load equals the resistance of the coil  $R_{coil}$  0.0680  $\Omega$  in order to maximize power transferred to the load. The electrical power was calculated in Equation 3:

$$P = \frac{V_{induced}^2}{4R_{coil}} = \frac{(N_{coil} \cdot 2\pi \cdot r_{coil} \cdot B_{radius} \cdot \frac{dd_{mag}}{dt})^2}{4R_{coil}} \quad (3)$$

where:  $V_{induced}$  is the voltage induced in the coil,  $R_{coil}$  is the resistance of the coil,  $N_{coil}$  is the number of coil turns,  $r_{coil}$  is the coil radius,  $B_{radius}$  is the magnetic flux density along the radius axis of magnetic spring,  $d_{mag}$  is the displacement of the levitated magnet in the magnetic spring.

In the calculations  $N_{coil}$  is set 1, considering the magnetic spring with single winding turn coil. The analysis is purely theoretical and simplified in order to investigate the better solution of the presence and absence the MR fluid in the energy harvester.

*Electrical power of magnetic spring prototype for middle magnet in the absence of MR fluid*

In Fig. 14a, for the input voltage of 6 V and for the frequency of 45 Hz, the highest power is  $1.82 \times 10^{-13} \text{ W}$ . In Figure 14b, for the input voltage of 4 V and for the frequency of 130 Hz, the

highest power is  $1.44 \times 10^{-14}$  W. In Figure 14c, for the input voltage of 4 V and for the frequency of 160 Hz, the highest power is  $4.75 \times 10^{-15}$  W.

#### *Electrical power of magnetic spring prototype for middle magnet in the presence of MR fluid*

In Figure 14a, for the input voltage of 6V and for the frequency of 35 Hz, the highest power is  $6.18 \times 10^{-12}$  W. In Figure 14 b, for the input voltage of 6V and for the frequency of 65 Hz, the highest power is  $1.39 \times 10^{-14}$  W. In Figure 14c, for the input voltage of 4 V and for the frequency of 150 Hz, the highest power is  $1.22 \times 10^{-18}$  W.

The magnetic spring in presence of MR fluid provides better electrical power efficiency in frequency range from 0 to 120 Hz. For the frequencies in range of 120 to 200 Hz for the input voltages of 4, 5 and 6 V, the power generated by the magnetic spring in the presence of the MR is lower than in the absence of the MR.

The MR fluid in the energy magnetic spring harvester contributes positively to the power enhancement for resonance frequencies and frequency tuning. The maximum power of magnetic spring prototype obtained in the presence of MR fluid for middle levitated magnet, as expected, is  $9.71 \times 10^{-12}$  W for the input voltage of 6 V and for the frequency of 35 Hz. The maximum power obtained in the absence of MR fluid is  $1.82 \times 10^{-13}$  W for the input voltage of 6 V and for the frequency of 45 Hz.

## CONCLUSIONS

In this article, a design of MR magnetic spring prototype was proposed, and analysis of its characteristic was investigated. In particular, the magnetic spring harvester subjected to external excitation of vibration generator was combined with MR fluid.

In order to verify its performance, a prototype was built with laboratory set-up providing the operating conditions in terms of frequencies and voltages that occur in environmental vibrations.

The potential of the device was estimated by the analysis of the magnetic flux density and displacements in the presence and in the absence of MR fluid. The MR fluid enhances the displacement of the levitated magnet in the range from 0 to 120 Hz with highest value of amplitude 0.12 mm. In terms of displacement, the usage of the MR

fluid is beneficial, as it increases the amplitude of the displacement in the wide range of frequency. The magnetic flux density in the magnetic spring in the presence of MR has the highest value of 3.07 mT in the range of frequency from 0 to 60 Hz. The magnetic spring in the presence of MR fluid provides better electrical power efficiency in frequency range from 0 to 120 Hz.

Certainly, many factors influence the properties of controllable MR fluids and magnets in the magnetic spring due to the vibration generator operating conditions, resonance frequencies and unstable amplitude of vibration. As a consequence, this study will contribute to the optimization of magnetic spring energy harvesting system to achieve more electric power, enhancing the magnetic flux density by the MR fluid and providing the wider range of working frequency.

## Acknowledgements

This research was supported by Subwencja na utrzymanie i rozwój potencjału badawczego, Politechnika Śląska. Magnetic spring with chambers filled with magnetorheological fluid (Sprężyna magnetyczna z wnękami wypełnionymi cieczą magnetoreologiczną). ZDI/2024/109. Centre for Incubation and Technology Transfer (CITT), Politechnika Śląska, Gliwice. Inventors: Grazia Lo Sciuto, Joanna Bijak and Zygmunt Kowalik. Submitted on 10th October 2024 with number P.450004

## REFERENCES

1. Sayed ET, Olabi AG, Alami AH, Radwan A, Mdallal A, Rezk A, et al. Renewable energy and energy storage systems. *Energies*. 2023; 16(3): 1415. <https://doi.org/10.3390/en16031415>
2. Ria A, Motroni A, Gagliardi F, Piotta M, Bruschi P. An IoT sensor platform for LED-based optical spectroscopy. In 2023 8th International Conference on Smart and Sustainable Technologies (SpliTech), 2023, June; 1–4, <https://doi.org/10.23919/SpliTech58164.2023.10193703>
3. Zheng X, He L, Wang S, Liu X, Liu R, Cheng G. A review of piezoelectric energy harvesters for harvesting wind energy. *Sensors and Actuators A: Physical*. 2023; 352: 114190. <https://doi.org/10.1016/j.sna.2023.114190>
4. Catania A, Gagliardi F, Piotta M, Bruschi P and Dei M. Ultralow-Power Inverter-Based Delta-Sigma Modulator for Wearable Applications, in *IEEE Access*, 2024; 12: 80009–80019, <https://doi.org/10.1109/ACCESS.2024.3388888>

- doi.org/10.1109/ACCESS.2024.3409842
5. Gagliardi F, Catania A, Ria A, Bruschi P, Piotta M. A compact all-MOSFETs PVT-compensated current reference with untrimmed 0.88%-( $\sigma/\mu$ ). In 2023 18th Conference on Ph. D Research in Microelectronics and Electronics (PRIME), 2023, June; 61–64, IEEE. <https://doi.org/10.1109/PRIME58259.2023.10161864>
  6. Gagliardi F, Ria A, Piotta M, Bruschi P. A 114 ppm/ $\circ$  C-TC 0.78%-( $\sigma/\mu$ ) Current Reference With Minimum-Current-Search Calibration. IEEE Transactions on Circuits and Systems II: Express Briefs., 2023, <https://doi.org/10.1109/TCSII.2023.3339586>
  7. Sun M, Song M, Wei G, Hua F. Electro-mechanical coupling analysis of l-shaped three-dimensional braided piezoelectric composites vibration energy harvester. Materials. 2024; 17(12): 2858. <https://doi.org/10.3390/ma17122858>
  8. Manikkavel A, Kumar V, Alam MN, Kim U, Park SS. The electro-mechanical energy harvesting configurations in different modes from machine to self-powered wearable electronics. ACS Applied Electronic Materials. 2023; 5(10): 5537–5554. <https://doi.org/10.1021/acsaelm.3c00819>
  9. Du R, Xiao J, Chang S, Zhao L, Wei K, Zhang W, et al. Mechanical energy harvesting in traffic environment and its application in smart transportation. Journal of Physics D: Applied Physics. 2023; 56(37): 373002. <https://doi.org/10.1088/1361-6463/acdadb>
  10. Panda S, Hajra S, Oh Y, Oh W, Lee J, Shin H, et al. Hybrid nanogenerators for ocean energy harvesting: mechanisms, designs, and applications. Small. 2023; 19(25): 2300847. <https://doi.org/10.1002/sml.202300847>
  11. Yu J, Li D, Li S, Xiang Z, He Z, Shang J, et al. Electromagnetic vibration energy harvester using magnetic fluid as lubricant and liquid spring. Energy Conversion and Management. 2023; 286: 117030. <https://doi.org/10.1016/j.enconman.2023.117030>
  12. Bahari MS, Firdaus M, Mohamed Z, Ramli MHM. Computational numerical analysis of a magnetic flux permanent magnet with different shape for the development of a hybrid generator. Journal of Mechanical Engineering (1823–5514). 2023; 20(1). <https://doi.org/10.24191/jmeche.v20i1.21087>
  13. Li B, Wang W, Li Z, Wei R. Hand-held rolling magnetic-spring energy harvester: Design, analysis, and experimental verification. Energy Conversion and Management. 2024; 301: 118022. <https://doi.org/10.1016/j.enconman.2023.118022>
  14. Deng L, Fan J, Gao X, Zhang Y, Fang Y, Wang D. Reducing the resonant frequency of the vibration energy harvester with a negative stiffness magnetic spring. IEEE Sensors Journal. 2024. <https://doi.org/10.1109/JSEN.2024.3407754>
  15. Royo-Silvestre I, Beato-L'opez J, G'omez-Polo C. Optimization procedure of low frequency vibration energy harvester based on magnetic levitation. Applied Energy. 2024; 360: 122778. <https://doi.org/10.1016/j.apenergy.2024.122778>
  16. Zhang X, Li G, Su S. Numerical and experimental performance study of magnetic levitation energy harvester with magnetic liquid for low-power-device's energy storage. Journal of Energy Storage. 2024; 75: 109584. <https://doi.org/10.1016/j.est.2023.109584>
  17. Fan B, Fang J, Jiang S, Li C, Shao J, Liu W. A hybrid energy harvester inspired by bionic flapping wing structure based on magnetic levitation. Review of Scientific Instruments. 2024; 95(1). <https://doi.org/10.1063/5.0178117>
  18. Hu C, Wang X, Wang Z, Wang S, Liu Y, Li Y. Electromagnetic vibrational energy harvester with targeted frequency-tuning capability based on magnetic levitation. Nanotechnology and Precision Engineering. 2024; 7(4). <https://doi.org/10.1063/10.0025788>
  19. Yu J, Yao J, Li D, Yu J, Xiao H, Zhang H, et al. A nonlinear electromagnetic vibration energy harvester lubricated by magnetic fluid for low-frequency vibration. Applied Physics Letters. 2023; 123(4). <https://doi.org/10.1063/5.0157431>
  20. Li C, Wu S, Luk PCK, Gu M, Jiao Z. Enhanced bandwidth nonlinear resonance electromagnetic human motion energy harvester using magnetic springs and ferrofluid. IEEE/ASME Transactions on Mechatronics. 2019; 24(2): 710–717. <https://doi.org/10.1109/TMECH.2019.2898405>
  21. Bahl S, Nagar H, Singh I, Sehgal S. Smart materials types, properties and applications: A review. Materials Today: Proceedings. 2020; 28: 1302–1306. <https://doi.org/10.1016/j.matpr.2020.04.505>
  22. Hua D, Liu X, Li Z, Fracz P, Hnydiuk-Stefan A, Li Z. A review on structural configurations of magnetorheological fluid based devices reported in 2018–2020. Frontiers in Materials. 2021; 8: 640102. <https://doi.org/10.3389/fmats.2021.640102>
  23. Skalski P, Kalita K. Role of magnetorheological fluids and elastomers in today's world. acta mechanica et automatica. 2017; 11(4): 267–274. <https://doi.org/10.1515/ama-2017-0041>
  24. Kowol P. From simple experiments to modern mechatronic devices-development of MR fluid applications. In: 2015 Selected Problems of Electrical Engineering and Electronics (WZEE). IEEE; 2015; 1–4. <https://doi.org/10.1109/WZEE.2015.7394022>
  25. Kowol P, Lo Sciuto G, Brociek R, Capizzi G. Magnetic Characterization of MR Fluid by Means of Neural Networks. Electronics. 2024; 13(9): 1723. <https://doi.org/10.3390/electronics13091723>
  26. Lo Sciuto G, Kowol P, Capizzi G. Modeling and experimental characterization of a clutch control

- strategy using a magnetorheological fluid. *Fluids*. 2023; 8(5): 145. <https://doi.org/10.3390/fluids8050145>
27. Yoon DS, Kim GW, Choi SB. Response time of magnetorheological dampers to current inputs in a semi-active suspension system: Modeling, control and sensitivity analysis. *Mechanical Systems and Signal Processing*. 2021; 146: 106999. <https://doi.org/10.1016/j.ymssp.2020.106999>
  28. Hua D, Liu X, Sun S, Sotelo MA, Li Z, Li W. A magnetorheological fluid-filled soft crawling robot with magnetic actuation. *IEEE/ASME Transactions on Mechatronics*. 2020; 25(6): 2700–2710. <https://doi.org/10.1109/TMECH.2020.2988049>
  29. Kun T, Hu S, Yinyun Y, Xuesong M. Magnetorheological fluid based force feed-back performance for main manipulator of invasive surgical robot. *Journal of Advanced Manufacturing Science and Technology*. 2022; 2(2). <https://doi.org/10.51393/j.jamst.2022007>
  30. Eshgarf H, Nadooshan AA, Raisi A. An overview on properties and applications of magnetorheological fluids: Dampers, batteries, valves and brakes. *Journal of Energy Storage*. 2022; 50: 104648. <https://doi.org/10.1016/j.est.2022.104648>
  31. Zhang G, Chen J, Zhang Z, Sun M, Yu Y, Wang J, et al. Analysis of magnetorheological clutch with double cup-shaped gap excited by Halbach array based on finite element method and experiment. *Smart Materials and Structures*. 2022; 31(7): 075008. <https://doi.org/10.1088/1361-665X/ac701a>
  32. Korona T, Kowol P, Lo Sciuto G. Design, manufacture and experimental characterization of magnetorheological rotary brake based on a peristaltic pump system. *Electrical Engineering*. 2023; 105(1): 435–446. <https://doi.org/10.1007/s00202-022-01675-5>
  33. Lo Sciuto G, Kowol P, Piłśniak A. Automated measurements and characterization of magnetic permeability in magnetorheological fluid. *Microfluidics and Nanofluidics*. 2022; 26(8): 55. <https://doi.org/10.1007/s10404-022-02565-9>
  34. Sikulskyi S, Malik A, Kim D. Magnetorheological Fluid Filled Spring for Variable Stiffness and Damping: Current and Potential Performance. *Frontiers in Materials*. 2022; 9: 856945. <https://doi.org/10.3389/fmats.2022.856945>
  35. Wang X, Zhang Y, Xue S, Wang T, Fu G, Mao X, et al. Bi-stable electromagnetic generator with asymmetrical potential wells for low frequency vibration energy harvesting. *Mechanical Systems and Signal Processing*. 2023; 199: 110478. <https://doi.org/10.1016/j.ymssp.2023.110478>
  36. Litak G, Kondratiuk M, Wolszczak P, Ambrożkiewicz B, Giri AM. Energy Harvester Based on a Rotational Pendulum Supported with FEM. *Applied Sciences*. 2024; 14(8): 3265. <https://doi.org/10.3390/app14083265>
  37. Lo Sciuto G, Bijak J, Kowalik Z, Kowol P, Brociek R, Capizzi G. Deep learning model for magnetic flux density prediction in magnetic spring on the vibration generator. *IEEE Access*. 2024. <https://doi.org/10.1109/ACCESS.2024.3406927>
  38. Bijak J, Sciuto GL, Kowalik Z, Lasek P, Szczygieł M, Trawiński T. Magnetic flux density analysis of magnetic spring in energy harvester by Hall-effect sensors and 2D magnetostatic FE model. *Journal of Magnetism and Magnetic Materials*. 2023; 579: 170796. <https://doi.org/10.1016/j.jmmm.2023.170796>
  39. Bijak J, Trawiński T, Szczygieł M. Simulation and investigation of the change of geometric parameters on voltage induced in the energy harvesting system with magnetic spring. *Electronics*. 2022; 11(10): 1639. <https://doi.org/10.3390/electronics11101639>
  40. Bijak J, Lo Sciuto G, Kowalik Z, Trawiński T, Szczygieł M. A 2-DoF kinematic chain analysis of a magnetic spring excited by vibration generator based on a neural network design for energy harvesting applications. *Inventions*. 2023; 8(1): 34. <https://doi.org/10.3390/inventions8010034>
  41. Lo Sciuto G, Bijak J, Kowalik Z, Szczygieł M, Trawiński T. Displacement and magnetic induction measurements of energy harvester system based on magnetic spring integrated in the electromagnetic vibration generator. *Journal of Vibration Engineering & Technologies*. 2024; 12(3): 3305–3320. <https://doi.org/10.1007/s42417-023-01045-w>